ACS Chemical Neuroscience

Research Article

pubs.acs.org/chemneuro

Nonoisotopic Assay for the Presynaptic Choline Transporter Reveals Capacity for Allosteric Modulation of Choline Uptake

Alicia M. Ruggiero,[†] Jane Wright,[†] Shawn M. Ferguson,[†,#] Michelle Lewis,[‡] Katie S. Emerson,[†] Hideki Iwamoto,[†] Michael T. Ivy,[∥] Ericka C. Holmstrand,[†] Elizabeth. A. Ennis,[†] C. David Weaver,[‡,⊥] and Randy D. Blakely*[,†,§]

[†]Center for Molecular Neuroscience, Department of Pharmacology, Vanderbilt University School of Medicine, Nashville, Tennessee 37232-8548, United States

[‡]Vanderbilt Institute of Chemical Biology, Vanderbilt University School of Medicine, Nashville, Tennessee 37232-6304, United States

[§]Department of Psychiatry, Vanderbilt University School of Medicine, Nashville, Tennessee 37232-8548, United States

[∥]Department of Biological Sciences, Tennessee State University, Nashville, Tennessee 37209-1561, United States

[⊥]Department of Pharmacology, Vanderbilt University School of Medicine, Nashville, Tennessee 37232-6600, United States

ABSTRACT: Current therapies to enhance CNS cholinergic function rely primarily on extracellular acetylcholinesterase (AChE) inhibition, a pharmacotherapeutic strategy that produces dose-limiting side effects. The Na^+-dependent, high-affinity choline transporter (CHT) is an unexplored target for cholinergic medication development. Although functional at the plasma membrane, CHT at steady-state is localized to synaptic vesicles such that vesicular fusion can support a biosynthetic response to neuronal excitation. To identify allosteric potentiators of CHT activity, we mapped endocytic sequences in the C-terminus of human CHT, identifying transporter mutants that exhibit significantly increased transport function. A stable HEK-293 cell line was generated from one of these mutants (CHT LV-AA) and used to establish a high-throughput screen (HTS) compatible assay based on the electrogenic nature of the transporter. We established that the addition of choline to these cells, at concentrations appropriate for high-affinity choline transport at presynaptic terminals, generates a hemicholinium-3 (HC-3)-sensitive, membrane depolarization that can be used for the screening of CHT inhibitors and activators. Using this assay, we discovered that staurosporine increased CHT LV-AA choline uptake activity, an effect mediated by a decrease in choline K_M with no change in V_{max}. As staurosporine did not change surface levels of CHT, nor inhibit HC-3 binding, we propose that its action is directly or indirectly allosteric in nature. Surprisingly, staurosporine reduced choline-induced membrane depolarization, suggesting that increased substrate coupling to ion gradients, arising at the expense of nonstoichiometric ion flow, accompanies a shift of CHT to a higher-affinity state. Our findings provide a new approach for the identification of CHT modulators that is compatible with high-throughput screening approaches and presents a novel model by which small molecules can enhance substrate flux through enhanced gradient coupling.

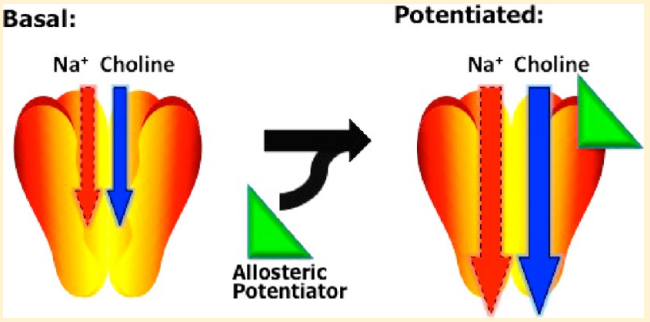

KEYWORDS: *Choline, transporter, hemicholinium-3, uptake, allosterism, assay, electrogenic*

Signaling by the neurotransmitter acetylcholine (ACh) controls a wide variety of physiological and behavioral functions throughout phylogeny, including movement, cardiovascular activity, gut motility, arousal, attention, and memory.[1−4] Genetic variation and/or deficits in components of cholinergic signaling are associated with myasthenias, tachycardia, attention-deficit hyperactivity disorder (ADHD), and Alzheimer's disease.[5−12] Medications that treat these disorders, though useful in some instances,[12−15] often exhibit dose-limiting side effects, are insufficiently specific, and generally act independently of neuronal activity. These effects are often found with agents that bind to the orthosteric site of intended targets. For example, muscarinic agonists that bind to the ACh binding site exhibit only modest selectivity among receptor subtypes and thus limit therapeutic efficacy.[16,17] Acetylcholinesterase (AChE) antagonists often produce many off-target effects due to elevation of ACh at all cholinergic synapses under conditions of both basal and evoked ACh release.[18] These issues underscore the need to identify novel cholinergic targets to ameliorate disorders with compromised ACh signaling.

An important molecule that controls cholinergic signaling capacity is the presynaptic, high-affinity choline transporter (CHT, *SLC5A7*). CHT activity is rate limiting in the synthesis of acetylcholine, particularly at elevated firing rates.[19−21] The

Received: June 24, 2012
Accepted: July 9, 2012
Published: July 9, 2012

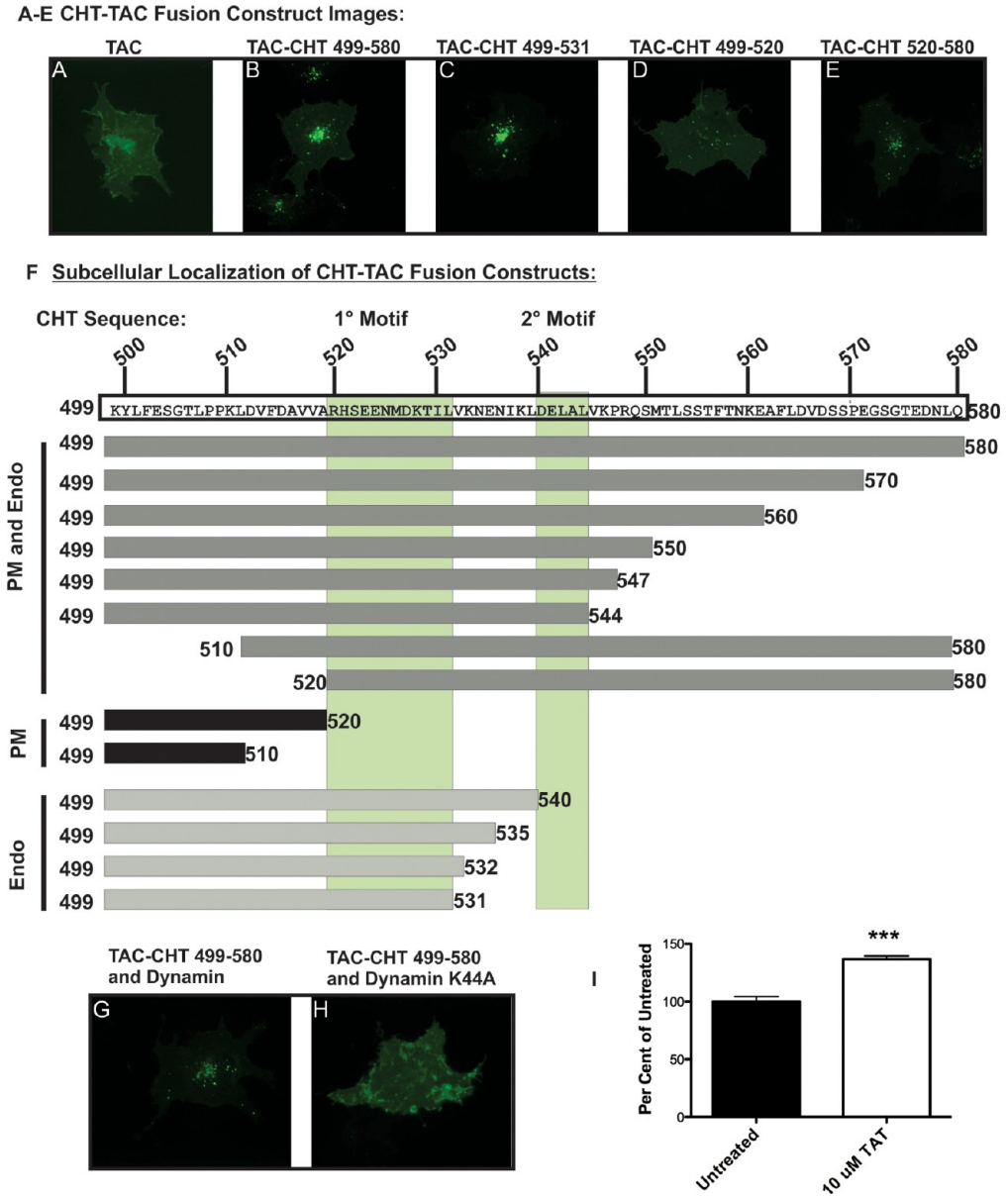

Figure 1. TAC−CHT fusion proteins indicate a discrete motif regulating CHT trafficking resides in the C-terminus. (A) Surface labeled Tac remains concentrated at the plasma membrane in HEK293 cells. (B) The full length CHT C-terminus directs internalization and sorting of the Tac-CHT chimera to a perinuclear endocytic compartment. (C) CHT amino acids 499−531 direct endocytosis when fused to Tac. This construct exhibits enhanced internalization compared to the full length CHT C-terminus. (D) Stable localization at the plasma membrane indicates that CHT amino acids 499−520 do not support efficient endocytic sorting of a Tac chimera. (E) Endocytic sorting of the Tac-CHT persists following deletion of CHT amino acids 498−519 (Tac-CHT520−580). (F) A summary of the localization of Tac-CHT deletion mutants presented in this figure points to CHT amino acids 522−532 as a 1° endocytic motif. A 2° motif appears between CHT amino acids 540−544 that facilitates CHT plasma membrane localization. (G) Cotransfection of WT dynamin I does not impair the endocytic sorting of Tac-CHT (Scale bar = 20 μm). (H) Expression of the dominant negative K44A mutant of dynamin I blocks internalization of the Tac-CHT chimera. (I) Saturation of the endocytic machinery by the CHT endocytic motif is seen as a 40% increase in CHT choline uptake activity following treatment of CHT expressing HEK293 cells with 10 μM of a CHT-TAT peptide fused to amino acids 524−539.

importance of CHT in sustaining cholinergic signaling can be readily observed in the lethality of systemic administration of the high-affinity CHT inhibitor hemicholinium-3 (HC-3)[22−24] or of genetic deletion of CHT.[25] CHT KO mice exhibit rundown of spontaneous and evoked cholinergic signaling at the neuromuscular junction and die at birth due to respiratory paralysis.[25] Patients with hypocholinergic function at the NMJ, at autonomic synapses, or within the central nervous system may therefore benefit from pharmacological augmentation of CHT function. Furthermore, by increasing CHT-dependent ACh synthesis, extracellular ACh levels will still be largely controlled by the rate of release and AChE activity. Many side-effects seen with AChE inhibitors could be abolished by the discovery of chemical agents that target CHT. To date, only one CHT-modulating agent, MKC-231, has been investigated as a potential therapeutic,[25−28] but its mechanism of action is ill-defined and likely does not involve a direct action on the transporter itself. These reports have however encouraged us to pursue targeting CHT for its therapeutic potential.

dx.doi.org/10.1021/cn3000718 | ACS Chem. Neurosci. 2012, 3, 767−781

The uptake of choline by CHT on the plasma membrane is generally assayed by monitoring the uptake of radiolabeled choline as a function of time in transfected cells or *ex vivo* brain preparations, such as synaptosomes.[26−29] These radioisotope-based methods are costly and generally incompatible with high-throughput screening (HTS) methods routinely used in drug development. Recently, Iwamoto and colleagues demonstrated that CHT is an electrogenic transporter that supports both choline-dependent and choline-independent net charge flux.[30] The current recorded in CHT expressing cells shares pharmacology with choline transport in being both Na^+- and Cl^--dependent and blocked by HC-3. Importantly, the current accompanying choline flux is nonstoichiometric, being ∼9-fold larger than the charge required to support gradient-driven choline transport. Thus, assays that monitor choline-induced membrane depolarization have the potential to provide an alternative to radiolabeled substrate flux-based methods that could facilitate HTS efforts.

In the current study, we pursue these ideas, describing our development of a membrane potential-based CHT assay that utilizes cells stably transfected with a CHT endocytic mutant. Our initial use of the assay in an HTS format reveals compounds that show differential impact on CHT-dependent choline uptake and CHT-dependent membrane depolarization, suggesting an opportunity for a novel mechanism of allosteric enhancement of membrane transporters in enhancing coupling to transmembrane ion gradients.

RESULTS AND DISCUSSION

Sequences in the Cytoplasmic C-Terminus of CHT Drive Constitutive Endocytosis. Although choline uptake studies monitor the activity of CHT at the cell surface where a Na^+ gradient is imposed, the transporter displays a significant accumulation on synaptic vesicles in neurons[29] or on synaptic-like microvesicles (SLMVs) and/or endosomes in transfected cell models.[31−33] In order to enhance CHT surface expression and enhance CHT activity in living cells, we sought to define sites in CHT responsible for constitutive CHT endocytosis. Mutants that limit endocytosis should also enhance the ability to target CHT allosterically and preclude an indirect manipulation of generic vesicular fusion/endocytosis machinery.

Our model of CHT transmembrane topology predicts a cytoplasmic localization for the transporter's C-terminus (AA# 498−580).[34] This prediction has been amply supported by biochemical and electron microscopy studies.[29,35,36] As the C-terminus is the longest, uninterrupted cytoplasmic region of CHT, it represents an attractive candidate for recognizing endocytic regulatory proteins. Additionally, analysis of the CHT C-term by the DisEMBL HOTLOOPS method[37] predicts a disordered structure for residues 522−580. Extended, disordered protein conformations are capable of engaging in multiple, dynamic, low-affinity interactions, a feature that is employed by multiple components of the endocytic machinery.[38] To test the capacity of the CHT C-terminus in supporting CHT endocytosis, chimeric proteins were generated by fusing the human CHT C-terminus to the N-terminal extracellular and transmembrane domains of the interleukin 2 receptor (also known as Tac).[39] The wild type (WT) Tac protein is frequently used to assess the endocytic capacity of membrane protein cytoplasmic domains as it demonstrates a low rate of constitutive endocytosis and can be labeled extracellularly with antibodies under nonpermeabilizing conditions.[40,41]

In initial experiments, we assessed the endocytosis activity of a Tac chimera containing the C-terminal 82 amino acids of CHT (CHT 499−580) relative to that shown by Tac lacking intracellular sequences. Transfected cells were labeled with anti-Tac antibodies at 4 °C, rinsed, and warmed to 37 °C to allow endocytosis of surface labeled proteins. The localization of chimeric proteins was determined using fluorescently conjugated secondary antibodies (see Methods). Tac-transfected cells displayed the expected labeling pattern, with immunofluorescence localized predominantly to the plasma membrane (Figure 1A). In contrast, labeling of cells transfected with Tac-CHT 499−580 revealed a predominant intracellular labeling (Figure 1B). Our conclusions regarding the limited endocytosis of Tac fusions are supported by findings that staining patterns following labeling at 4 °C followed by rewarming to 37 °C is the same as those detected when labeling is visualized immediately following labeling at 4 °C or if the permeabilization step is omitted altogether (data not shown). Conversely, the punctate labeling of Tac-CHT 499−580 following surface labeling and rewarming requires permeabilization for detection as expected for the fusion's relocation to an intracellular compartment rather than clustering on the plasma membrane.

To map the location of sequences directing endocytosis of the Tac-CHT 499−580 chimera, we generated and analyzed Tac constructs bearing overlapping deletions of the CHT C-terminus (representative images, Figure 1C−E; a summary of the localization of all mutants is presented in Figure 1F). Deletions of up to 36 amino acids (Tac-CHT 498−544) from the CHT C-terminus failed to alter the gross, intracellular localization of Tac C-terminal chimeras, whereas deletions of between 40 (Tac-CHT 499−540) and 48 amino acids (Tac-CHT 499−532) yielded results consistent with enhanced delivery of chimeras to intracellular compartments (Figure 1C). In contrast, a Tac fusion bearing a C-terminal 60 amino acid deletion (Tac-CHT 498−520) (Figure 1D) demonstrated a pattern of prominent surface labeling much like that of Tac protein lacking fused sequences. Analysis of a Tac fusion bearing a more N-terminal deletion revealed that loss of the membrane-adjacent 21 amino acids of the CHT C-terminus (Tac-CHT 520−580) supports efficient Tac-CHT endocytosis (Figure 1E). When analyzed together, these deletions define a discrete region between amino acids S522 to V532 (SEENMDKTILV-1° Motif) of the CHT C-terminus that drive endocytosis of Tac (Figure 1F). Additionally, these studies identify another sequence motif between D540 and L544 (DELAL-2° Motif) that supports enhanced surface expression of the Tac-CHT fusion. However, in the context of a full C-terminus, or in the full length CHT (see below), this secondary motif does not appear to exhibit a dominant capacity for surface trafficking.

Previously, we reported that coexpression of WT CHT with dynamin I−K44A, a dominant-negative inhibitor of dynamin-dependent endocytosis,[42,43]significantly elevated the cell surface expression of CHT.[44] To determine whether the C-terminus of CHT supports dynamin-dependent endocytosis, we tested the effect of the K44A mutant on Tac-CHT 499−580. Whereas coexpression of wild type dynamin 1 had no effect on the internalization capacity of Tac-CHT 499−580 (Figure 1G), dynamin 1-K44A coexpression blocked the endocytosis of Tac-CHT 499−580 (Figure 1H). If CHT C-terminal sequences are essential for CHT endocytosis, then CHT C-terminus peptides may block internalization of full length CHT by competing with essential endocytic proteins and thereby elevating choline uptake activity. Indeed, we measured a 30% increase in choline transport

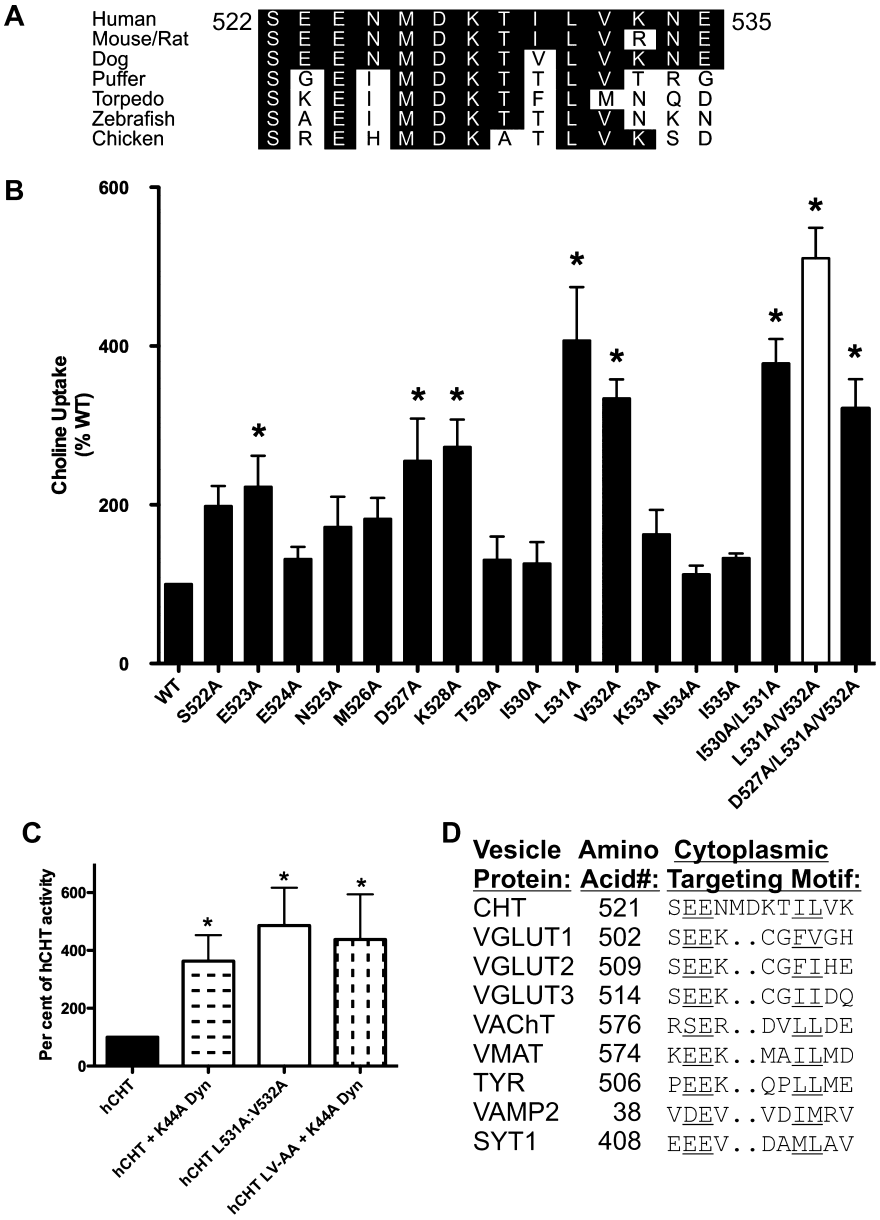

Figure 2. Characterization of the CHT endocytosis motif by alanine-scanning mutagenesis. (A) The 1° endocytic sequence motif of CHT identified in Figure 1 is conserved across multiple species. (B) Analysis of choline transport in transiently transfected COS-7 cells reveals that alanine substitution of specific CHT residues within this interval results in a significant increase in CHT-mediated choline transport (*$p < 0.05$ by ANOVA followed by Bonferroni's post-test; $n = 4–7$ for each mutant). The L531A mutation gave the greatest single residue mutation uptake increase. The combined L531A and V532A combination gave the greatest uptake increase. This mutant was chosen for further characterization, referred to as CHT LV-AA in text. (C) The cotransfection of a dominant negative mutant of dynamin (K44A) does not contribute to additional increases in the activity of CHT mutants within the basal endocytic motif. (D) The sequence of 522–532 in CHT has elements in common with the characterized targeting sequence of other synaptic vesicle proteins, specifically the dileucine-type motif identified as the most active CHT mutation.[46,69].

activity following treatment of CHT expressing cells with a TAT-fusion peptide for the CHT C-terminus 1° Motif (Figure 1I). The transctivating transcriptional activating (TAT) peptide sequence from HIV-1 is a cell penetrating peptide sequence that facilitates internalization of peptides.

Site-Directed Mutagenesis of CHT to Identify Key Residues Supporting Basal Endocytosis. Amino acids within the CHT C-terminus are not well conserved between mammals and invertebrates.[45] However, substantial conservation is evident across the region comprising CHT amino acids 522–535 (Figure 2A), a region that overlaps with the region we designated as the 1° endocytic determinant motif for CHT in either COS-7 or HEK293 cells. To identify specific amino acids within this region that accounts for efficient endocytosis, we implemented an alanine-scanning mutagenesis approach, evaluating the functional effects of mutations on CHT via assessment of choline uptake (Figure 2B). In comparison to the activity of WT CHT, transporters bearing alanine substitutions at positions 522, 523, 527, 528, 531, and 532 produced statistically significant increases in choline uptake. Alanine substitution at the highly conserved residue L531 yielded the largest single effect in these experiments. The double mutations I530A/L531A and the triple mutation D527A/K528A/L531A did not significantly increase CHT-mediated choline uptake beyond that elicited by the single

dx.doi.org/10.1021/cn3000718 | ACS Chem. Neurosci. 2012, 3, 767–781

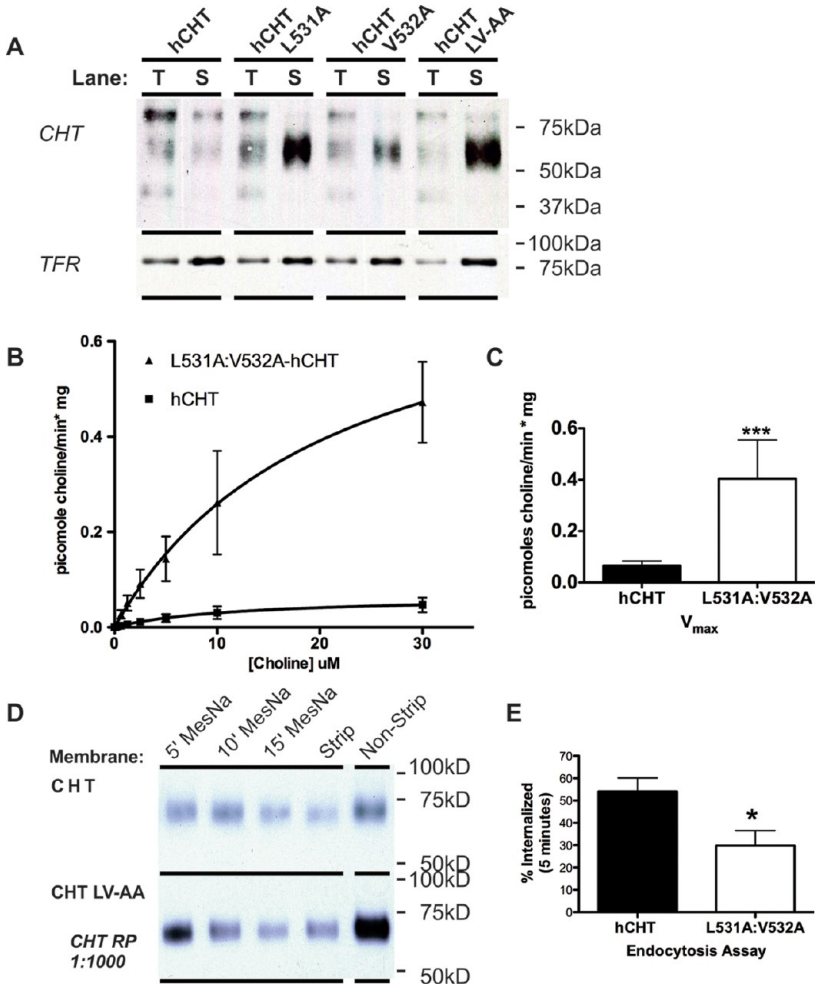

Figure 3. Characterization of the L531A/V532A CHT (LV-AA) mutant in transiently transfected cell lines. (A) Comparison of cell surface residence among CHT, L531A, V532A, and LV-AA CHT in transiently transfected COS-7 cells. Following cell surface biotinylation, total (T) or surface (S) fractions or the wild type and each mutant CHT were examined. The total fractions represent 10% of the input into the biotinylated protein extractions. (B) Saturation kinetic analysis of CHT LV-AA compared to WT CHT was performed in transiently transfected COS-7 cells. CHT LV-AA has a significant increase in activity compared to WT CHT (two way ANOVA interaction *P*-value <0.001 to 0.003). (C) The measured V_{max} was 0.0676 ± 00841 pmol choline/min·mg for WT CHT versus 0.463 ± 00.119 pmol choline/min·mg for CHT LV-AA ($p = 0.0006$, $n = 5$, two way ANOVA). The K_M was not significantly altered by the mutation (data not shown), 10.58 ± 4.287 μM for WT CHT versus 7.484 ± 2.581 μM for CHT LV-AA (Student's *t* test). (D) Biotinylation-stripping endocytosis assay by treatment with MesNa after incubation at 37 °C for 5−15 min shows a greater level CHT LV-AA maintained on the cell surface than WT CHT. (E) Quantification of internalization at 5 min finds an impact of the LV-AA CHT mutation as a reduction in the percent internalized protein compared to the WT CHT ($p = 0.03$, $n = 3$, Student's *t*-test).

L531A mutation. However, the double substitution L531A/V532A (white bar) generated even higher levels of uptake activity than either substitution alone. Importantly, the increase in choline transport activity found for the LV mutant was not further augmented by cotransfection with the dynamin mutant K44A, consistent with participation of the LV sequences in dynamin-dependent, constitutive endocytosis of CHT (Figure 2C). When examined in comparison with other transporters that exhibit efficient endocytosis, and a localization to synaptic vesicles, the CHT LV sequence can be seen to lie within a conserved dileucine-type motif, preceded by a cluster of acidic residues[46] (Figure 2D). Therefore, in subsequent experiments we pursued a further analysis of endocytosis of the "CHT LV-AA" mutant and used it to develop a HTS-compatible assay of CHT activity.

CHT LV-AA Mutation Reduces Constitutive CHT Endocytosis and Choline Transport Capacity. If the LV-AA mutation in full-length CHT elevates choline uptake activity via a disruption of constitutive CHT endocytosis, we should detect an increase in steady-state levels of plasma membrane CHT. To explore this issue, we employed cell-surface biotinylation, comparing WT (wild type) CHT and CHT LV-AA in transiently HEK-293T transfected cells. As predicted, CHT LV-AA exhibited a significant increase in CHT cell-surface expression compared to WT CHT (Figure 3A). Expression of CHT LV-AA did not impact plasma membrane abundance of the transferrin receptor, a protein known to constitutively recycle by clathrin-mediated endocytosis,[47] indicating that the mutant transporter does not exert a general effect on constitutive endocytic proteins. The lack of calnexin in biotinylated extracts demonstrates that surface fractions were not contaminated with intracellular proteins (data not shown).

Kinetic analysis of choline uptake by CHT LV-AA in transiently transfected cells confirmed expectations from biotinylation experiments, as we detected an increase in choline uptake V_{max} but not in choline K_M (Figure 3B−C and Table 2).

dx.doi.org/10.1021/cn3000718 | *ACS Chem. Neurosci.* 2012, 3, 767−781

Table 1. Alterations in V_{max} in Saturation Kinetic Studies of CHT and LV-AA Following PMA and Staurosporine Treatment of the HEK293 Stable Cell Line[a]

cell line	treatment	V_{max} (mean ± SEM)	fold change
hCHT	none	1.95 ± 0.50	
hCHT LV-AA	none	6.20 ±1.42(**)	3.2-fold increase from WT CHT
hCHT	PMA (1 μM)	0.624 ± 0.11(***)	2.6-fold decrease from untreated WT
hCHT LV-AA	PMA (1 μM)	3.52 ± 0.40(*)	1.8-fold decrease from untreated LV
hCHT	Stauro. (5 μM)	1.35 ± 0.28(*)	1.4-fold decrease from untreated WT
hCHT LV-AA	Stauro. (5 μM)	6.21 ± 0.97	

[a]Treatment with PMA reduced the V_{max} of both the CHT and CHT LV-AA cell lines. Treatment with staurosporine did not have a significant impact on the V_{max} of CHT LV-AA but did reduce the V_{max} of CHT. These measurements are the combined analysis of an $n = 4–5$ trials in triplicate. Significant change was determined by Student's *t*-test analysis of all trials and reported next to values as *–*** for *p* values less than 0.5–0.01. Standard error between replicates is less than 10% (data not shown).

Table 2. Alterations in K_M in Saturation Kinetic Studies of CHT and LV-AA Following PMA and Staurosporine Treatment of the HEK293 Stable Cell Line[a]

cell line	treatment	K_M (mean ± SEM)	fold change
hCHT	none	19.26 ± 9.1	
hCHT LV-AA	none	21.13 ± 9.0	
hCHT	PMA (1 μM)	9.72 ± 4.3(*)	1.98-fold decrease from untreated WT
hCHT LV-AA	PMA (1 μM)	17.3 ± 4.1	
hCHT	Stauro. (5 μM)	4.45 ± 2.8(**)	4.3-fold decrease from untreated WT
hCHT LV-AA	Stauro. (5 μM)	11.91 ± 4.4(*)	1.7-fold decrease from untreated LV

[a]Treatment with PMA had a significant impact on K_M of the CHT cell line. Treatment with staurosporine reduced the K_M of both the CHT and the CHT LV-AA cell lines. These results imply that the uptake increases measured with staurosporine are not due to increased trafficking of the transporter but are more likely due to an increase in kinetic efficiency of the transporter. These measurements are the combined analysis of $n = 4–5$ trials in triplicate. Significant change was determined by Student's *t*-test analysis of all trials and reported next to values as *–*** for *p* values less than 0.5–0.01. Standard error between replicates is less than 10% (data not shown).

To determine whether the elevated surface expression and enhanced transport V_{max} were derived from reduced rates of endocytosis, we performed MesNa stripping experiments that assess the time-dependent residence of membrane proteins after surface labeling. These studies (Figure 3D,E) revealed that rates of constitutive endocytosis of CHT LV-AA are significantly reduced in comparison with CHT WT. These findings parallel our observations using dynamin dominant–negative cotransfections and support the elevation in choline uptake and endocytic capacity as arising from a perturbation of dynamin-dependent, CHT endocytosis. Our findings are also consistent with evidence that disruption of the AP3 adaptor complex in the *mocha* mouse[31] results in accumulation of CHT in the cell soma of cholinergic neurons since AP3 machinery is involved in dileucine-motif-based vesicle budding for somatic export.[48] AP3 plays a role in the plasma membrane recycling of other vesicular proteins at synaptic terminals, such as VGLUT isoforms.[48,49]

Saturation Kinetic Studies of CHT Regulation in Stable Cell Lines. To explore whether small molecule regulators of CHT can exert comparable influences over CHT LV-AA as seen with WT CHT, we generated stable HEK-293 cell lines expressing either transporter. After identifying clones with comparable transporter protein expression levels, as assessed by immunoblots of total cell extracts, we observed the expected elevation of CHT activity for the CHT LV-AA line and found the elevated functional expression to derive from elevated transporter surface expression (Figure 4A,B). Consistent with these findings, the V_{max} of choline uptake was found to be significantly elevated in CHT LV-AA cells, without a change in choline K_M (see Tables 1–2).

Phosphorylation of multiple, presynaptic proteins (e.g., synapsin) is critical for synaptic vesicle release and endocytosis in response to depolarization-induced elevations in intracellular calcium.[50–52] In relation to this study, synaptosomal CHT activity and plasma membrane levels have been reported to be regulated by protein kinase C (PKC) and cAMP-dependent kinase (PKA)-linked pathways.[53–55] In our stable cells expressing WT CHT, application of the PKC activator PMA (1 μM, 10 min) reduced choline uptake, arising from a reduction in both the choline K_M and choline transport V_{max} (Figure 4C,D). Surface expression of WT CHT in these cells was too low to reliably detect a reduced surface expression under conditions of a reduced V_{max}, though this change seems likely. Importantly, a V_{max} change was also apparent when cells expressing the CHT LV-AA mutant were treated with PMA (Figure 4C), and here the elevated steady-state transporter surface expression allowed us to detect a reduction in CHT LV-AA surface expression (Figure 4G,H). Thus, although the CHT LV-AA mutant displays a significant change in basal endocytosis capacity, PKC-dependent regulatory mechanisms can still enhance internalization of transporters, suggesting that additional endocytic motifs/pathways participate in this regulation. Interestingly, a choline K_M reduction was observed with PMA treatment of WT CHT after PMA treatment that was not observed in CHT LV-AA experiments. A reduction in choline K_M suggests a shift in one or more CHT conformations that increase CHT affinity for substrate. One mechanism that could explain these findings is that normally, following PKC activation, CHT shifts from a constitutive endocytosis pathway to a regulated pathway. With this shift could come an exchange of different associated proteins that stabilize distinct CHT conformations linked to choline interactions, read out in saturation transport assays as a change in K_M. Ramamoorthy's group has identified a K_M shift in serotonin transport in platelets after PMA application, accompanied by a distinct pattern of serotonin transporter (SERT) phosphorylation than observed later once SERT moves into a PKC-dependent, endocytic pathway. Possibly, the CHT LV-AA mutation may not permit post-translational modifications and/or protein associations that are needed to enter a PKC-dependent, endocytic pathway, and precluding the shift of choline K_M seen with WT CHT. We recently identified a mutant dopamine transporter (DAT) derived from a subject with Attention Deficit/Hyperactivity Disorder (ADHD) that exhibits an altered ability to adopt normal protein associations and trafficking itineraries.[56] These findings raise the possibility that alterations mimicking the changes observed with the CHT LV-

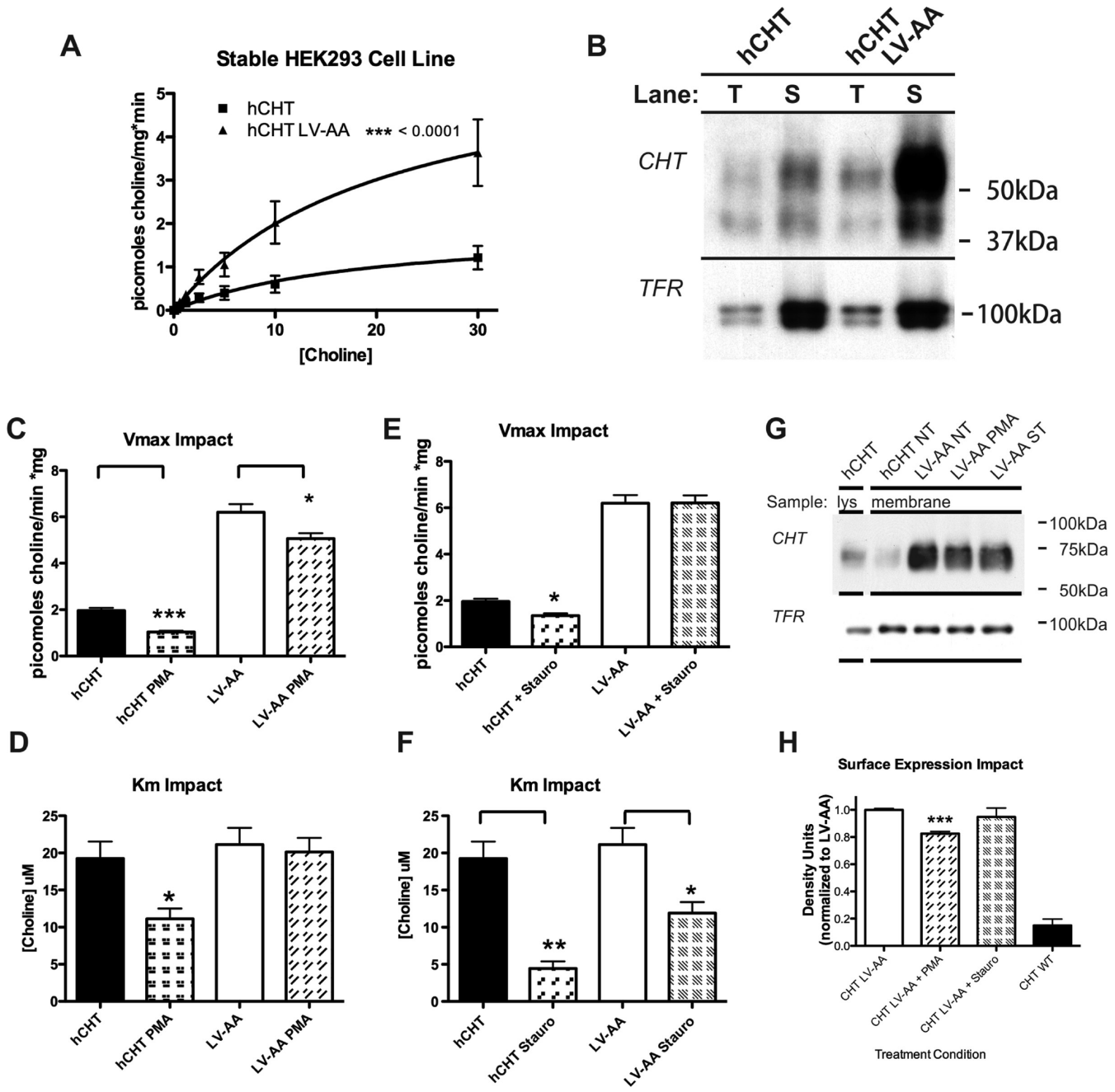

Figure 4. Generation of CHT expressing stable cell lines to facilitate HTS development. HEK293 cell lines were generated expressing CHT and the LV-AA mutant. (B) The expression of WT CHT and CHT LV-AA was characterized by saturation kinetic analysis. LV-AA CHT demonstrates a 3-fold increase in V_{max} (see Tables 1−2). (A) These cell lines were analyzed for cell surface expression by membrane impermeant biotinylation; again as shown for the transient expression, LV-AA CHT has a much greater cell surface expression. (C−D) Saturation kinetic analysis of the cell lines was performed under the condition of no treatment and PMA treatment to activate PKC. The PMA treatment reduced measured V_{max}. (E−F) Saturation kinetic analysis was performed under the condition of staurosporine treatment to inhibit kinase activity. The predominant effect was a reduction in measured K_M. (G−H) The surface trafficking impact of PMA and staurosporine treatment was examined using membrane impermeant cell surface biotinylation in the CHT LV-AA cell line. Treatment of the cell line with PMA, but not staurosporine, leads to a significant reduction in cell surface expression (p = 0.0005, n = 3, Student t-test).

AA mutation may contribute to disorders linked to compromised cholinergic signaling.

Since PMA reduces choline transport capacity in parallel with enhanced transporter endocytosis with either WT CHT or CHT LV-AA cells, it seems likely that the sequences that mediate PKC-dependent transporter down-regulation lie distal to the LV dileucine motif. S522 in CHT corresponds to S480 in VAChT (see Figure 2D). S480 is phosphorylated in response to PKC activation,[57] with an accompanying reduction in VAChT localization to synaptic vesicles. We have found that the CHT S522A mutant supports equivalent choline transport activity as WT CHT (data not shown). Moreover, these transporters are equally sensitive to PMA treatments (data not shown, n = 5, p < 0.05 t-test). Similar sensitivity was also observed with a T529A substitution. These findings support the idea that constitutive and PKC-induced CHT endocytosis derive from distinct

dx.doi.org/10.1021/cn3000718 | ACS Chem. Neurosci. 2012, 3, 767−781

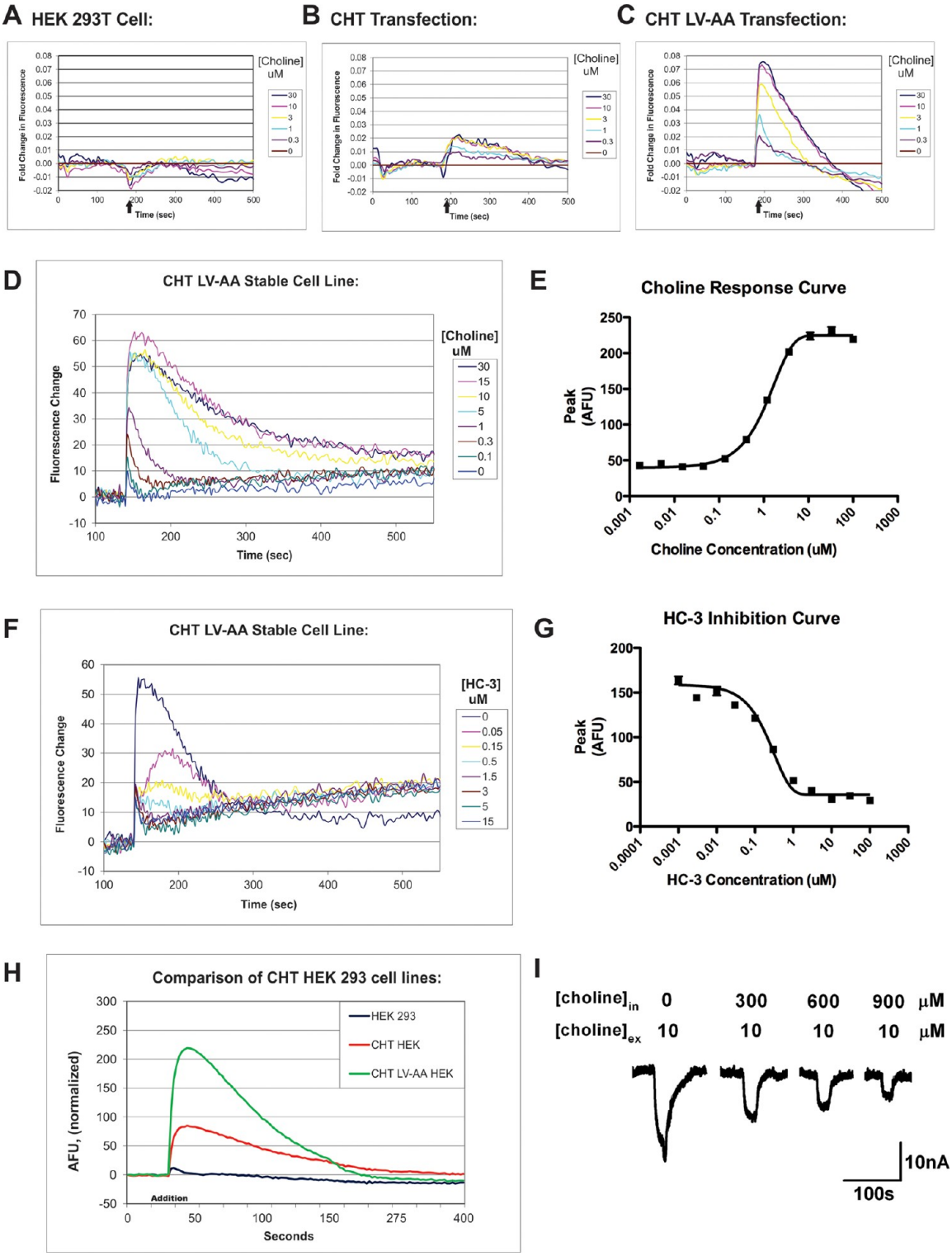

Figure 5. Development of the CHT HTS assay using membrane-potential sensitive fluorescent dyes (Molecular Devices). Membrane potential sensitive dyes are incubated with HEK293 cells that are monitored in real time for fluorescent signal changes. (A) HEK293 cells do not generate a fluorescent signal following the application of choline (black arrow) and therefore do not demonstrate a choline-induced depolarization. (B–C) Transient transfection of WT CHT and CHT LV-AA into HEK293T cells demonstrated a specific choline-induced depolarization signal. (D–E) The LV-AA CHT stable cell line displayed an improved signal-to-noise ratio and a linear choline concentration–response from 0.1 to 30 μM. The signal measured using CHT LV-AA cells was significant enough to consider for the creation of a HTS assay to uncover allosteric potentiators of CHT. (F–G) The specific CHT antagonist HC-3 inhibits the choline-induced membrane depolarization of this cell line. (H) Summary comparison of the relative signal response of HEK293 cell lines expressing WT CHT and CHT LV-AA to choline-induced membrane depolarization. (I) CHT LV-AA expressing oocyte membrane current response to choline is reduced under conditions of very high internal choline concentrations.[30].

dx.doi.org/10.1021/cn3000718 | ACS Chem. Neurosci. 2012, 3, 767–781

mechanisms. Similar conclusions have been reached regarding sequences supporting the basal and PKC-dependent endocytosis of DAT.[58,59]

Gates and colleagues found that the broad specificity kinase inhibitor staurosporine produced no effects on its own in rat synaptosomes at 1 μM but blocked PMA-induced reductions in choline uptake.[53] We were thus surprised to find that treatment of WT CHT stable cells with staurosporine (5 μM, 10 min) produced a 2-fold increase in choline uptake ($n = 16$, $p < 0.005$ t-test, Figure 7B) that was supported by a significant reduction in choline K_M (Figure 4E,F). These findings are consistent with a staurosporine-induced alteration in choline affinity. A reduction in WT CHT V_{max} was also observed after staurosporine treatment (see Tables 1−2). As noted for PMA studies, levels of WT CHT surface expression were insufficient to determine whether V_{max} reductions derive from a reduction in transporter surface expression. Additionally, when we treated isolated mouse striatal synaptosomes with staurosporine (5 μM, 10 min), we measured a significant increase in choline uptake, when measured at sub-K_M concentrations, though to not as large an extent as seen in the cell culture models (Figure 7F,G). Gates and colleagues[53] used a preparation of combined hippocampal and striatal synaptosomes. We did not observe a stimulation of CHT activity in hippocampal synaptosomes, and thus, the differences in the Gates study and ours suggest region-dependent differences in CHT conformations or signaling pathways that support sensitivity of CHT to staurosporine. In contrast to staurosporine, we found that the more specific PKC inhibitor BIM-1 did not stimulate CHT uptake (data not shown)). Thus, staurosporine appears to shift CHT K_M via a PKC-independent mechanism. Staurosporine also produced a reduction in choline transport K_M in CHT LV-AA cells. However, CHT LV-AA cells did not display the reduced V_{max} seen with WT CHT cells (Figure 4E,F), nor did we detect a significant reduction in CHT LV-AA surface expression following staurosporine treatment (Figure 4H). On the basis of these observations, we hypothesize that the actions of staurosporine are allosteric in nature, either through a direct interaction with CHT or through the action of a CHT modulator, where both WT CHT and CHT LV-AA can be shifted to a high-affinity state. In the case of WT CHT, an accompanying reduction in CHT V_{max} can offset the K_M effect when assays are performed at higher concentrations of choline, thereby obscuring an effect of staurosporine on transport function. If the allosteric hypothesis for the actions of staurosporine is correct, molecules developed around a staurosporine scaffold could act to sustain choline transport activity when levels of uptake are limited by extracellular choline availability.

Development of a Nonisotopic, HTS-Compatible Assay of CHT Function. The development of CHT LV-AA cells that exhibit significantly diminished constitutive endocytosis and our studies with staurosporine encouraged our development of an HTS-compatible assay for allosteric potentiators/inhibitors. As noted above, however, measurement of radiolabeled choline flux is expensive and less suitable for the automation needed in HTS efforts compared to nonradioisotopic techniques. Interestingly, CHT has been demonstrated to be an electrogenic transporter, demonstrating choline-independent (i.e., "leak") and choline-dependent currents, both of which are blocked by HC-3.[30] Additionally, the latter studies demonstrated a significantly elevated choline-induced current in human CHT LV-AA cRNA-injected *Xenopus* oocytes, as compared to WT CHT. We hypothesized that if these currents are evident in our transfected mammalian cells, then we may be able to utilize voltage-sensitive dyes to follow membrane depolarization as an HTS-compatible surrogate for CHT activity. To assess this possibility, we utilized transient transfection of WT CHT and the CHT LV-AA in HEK293T cells, monitoring membrane potential-dependent changes in fluorescence in a 384-well plate format. As shown in Figure 5A, untransfected HEK293T cells do not exhibit a measurable depolarization following choline (10 μM) addition. Addition of choline to WT CHT-transfected cells produced only a small increase in fluorescence above that seen with non-transfected cells (Figure 5B), even at saturating choline concentrations. However, and as predicted from [^{3}H]-choline transport assays, choline application to CHT LV-AA transfected cells produced a much larger, dose-dependent, membrane depolarization (Figure 5C). Although the depolarization-dependent signal rose rapidly following choline application, the fluorescence signal waned despite the continued presence of choline. Importantly, depolarizations induced by choline in both WT CHT and CHT LV-AA transfected cells were inhibited by HC-3 at potencies expected from transport assays (data not shown).

Using the CHT LV-AA stable cell lines, we pursued a more thorough characterization of CHT-associated membrane depolarization, pursuant to its use for HTS activities. As with transiently transfected cells, stable CHT LV-AA cells displayed a dose-dependent, choline-induced membrane depolarization that exhibited a rapid rise to peak signal after choline application followed by a slower decline to baseline. When peak signals were monitored as a function of choline, we obtained data that could be well fit to a 1 site model, yielding a K_M of choline of 3.11 ± 1.19 μM, close to the choline K_M values obtained with radiometric assays (Table 1). HC-3 inhibited choline-induced depolarization of CHT LV-AA cells with an IC_{50} of 320 nM, which after transformation[60] yields a K_I of ∼10 nM, similar to cholinergic nerve terminals where an IC_{50} for HC-3 of ∼50 nM has been reported.[61,62] Together, these findings indicate that assays in stably transfected CHT LV-AA cells can be a useful, HTS-compatible substitute for traditional CHT assays employing radiotracer methods.

The transient nature of CHT LV-AA membrane depolarization following choline application could arise from transporter inactivation or internalization. Okuda and colleagues[63] recently reported that choline could induce CHT internalization, though not over the time course needed to account for our transient changes in membrane depolarization. Moreover, our own biotinylation studies did not reveal choline-induced alterations in CHT surface expression in stably transfected HEK-293T cells (data not shown). Possibly, the transient nature of the fluorescence signal could derive from a time-dependent reduction in the ion/substrate gradients needed to sustain continued net choline-induced charge flux. Once the concentration of intracellular choline reaches the equilibrium value permitted by the electrochemical gradient driving choline uptake, net CHT activity will cease. We tested this idea using CHT LV-injected *Xenopus laevis* oocytes, where we monitored choline-inducted currents after injections of choline to mimic the increasing intracellular concentrations of our stable cells. We found that CHT-induced currents declined as internal choline concentrations rose (Figure 5I), consistent with the transient nature of the CHT-dependent current as arising from accumulation of intracellular choline. These data also argue for the use of peak depolarization as the dependent measure when

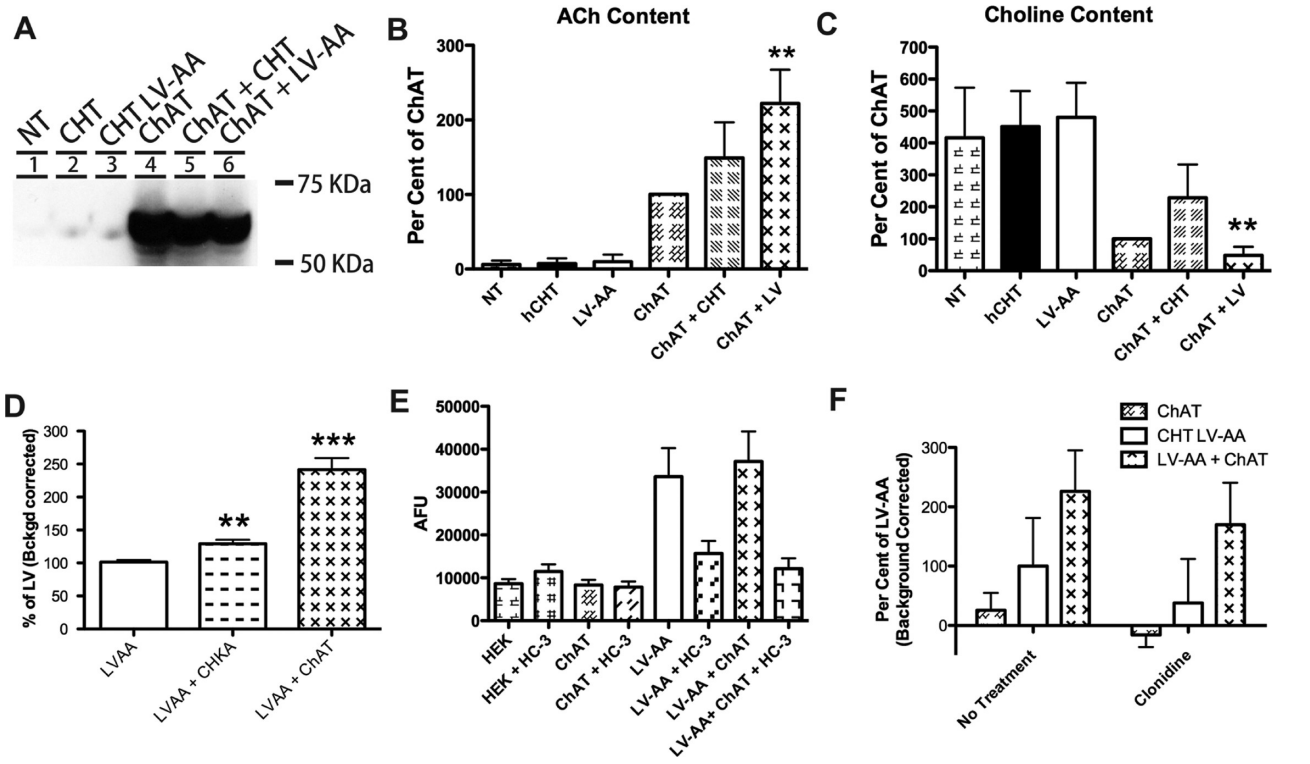

Figure 6. Investigation of auxiliary methods to increase choline-induced membrane potential to facilitate the HTS screen. (A) The cholinergic enzyme choline acetyltransferase (ChAT) synthesizes acetylcholine (ACh) from choline. ChAT was transiently transfected into HEK293T cells and produced the cytoplasmic protein. (B) ChAT transfected in HEK293T cells was capable of producing ACh as measured by HPLC analysis. (C) ChAT transfection into HEK293 cells reduced the basal choline level of the cells (**$n = 4$, $p < 0.01$). (D) The choline utilizing enzymes, CHKA and ChAT, significantly increased ^{3}H-choline uptake in cotransfected HEK293T cells (***$n = 6$, $p < 0.001$). (E) The cotransfection of LV-AA CHT (white bar) with ChAT (X-hatch bar) did not increase the response to the choline-induced membrane potential assay. (F) Inhibition of the organic cation transport (OCT) system with clonidine[65] reduced the ^{3}H-choline uptake increase seen following ChAT cotransfection with CHT LV-AA. Significant change was determined by Student's *t*-test analyses of all trials $n = 3–5$ for all assays and reported under values as *–*** for p values less than 0.05–0.001.

using the fluorescence assay for quantitative analyses of CHT modulation.

Given the inhibitory effects of intracellular choline noted on CHT-dependent ion flux, we pursued approaches to increase the driving force for choline entry, with an eye to increasing further CHT activity signals as an aid to HTS efforts. We reasoned that metabolism of intracellular choline during the assay could maintain the driving force for choline uptake since a component of that driving force is choline itself. Therefore, we cotransfected cDNAs encoding the enzyme choline acetyl-transferase (ChAT) along with either WT-CHT or CHT LV-AA, and then assessed the impact on choline uptake relative to cells transfected with the transporters alone. We verified expression of ChAT protein by Western blot (Figure 6A) and established that expression of ChAT in HEK293T cells led to the production of ACh by HPLC (Figure 6B). We also determined that transfected ChAT consumed sufficient choline to reduce the endogenous choline content by ~3-fold when compared to cells transfected with CHT LV-AA alone (Figure 6C). As predicted, ChAT cotransfection with CHT LV-AA significantly increased choline uptake by 2.5-fold (Figure 6D). Similarly, cotransfection of choline kinase L (CHKL) or choline kinase A (CHKA) (data not shown), other enzymes that utilize choline as a substrate, also led to a significant increase in choline uptake (**$n = 6$, $p < 0.01$).

Surprisingly, these treatments did not alter choline-induced membrane potential changes (Figure 6E). Since the membrane potential assay we used is likely driven by CHT-dependent sodium flux, we reasoned that the failure to produce enhanced membrane depolarization despite elevated choline uptake could derive from endogenous electroneutral choline transport pathways. Organic cation transport systems are expressed in HEK293 cells,[64] and these transporters that could be responsible for the elevation in choline flux rates observed when endogenous choline levels are depleted. Supporting these ideas, incubation of ChAT/CHT LV cotransfected cells with the OCT2 inhibitor clonidine[65] (Figure 6F) reduced the gain achieved in choline uptake relative to CHT LV-AA cells. Together, these data indicate that reducing intracellular choline to achieve higher choline transport rates in HEK293 cells obfuscates contributions of choline uptake by CHT. Importantly, the electroneutral nature of these pathways suggests that we are unlikely to recover false-positve, small molecules in HTS screens of CHT-supported membrane depolarization. Further studies are required to understand why intracellular choline injections influenced CHT-dependent currents in *Xenopus laevis* oocytes, though this may derive from lower endogenous expression of electroneutral choline transport pathways in *Xenopus* oocytes[66] compared to that in HEK293T cells, thereby allowing choline levels to more specifically alter CHT function.

CHT Activator Staurosporine Reduces Choline-Induced Membrane Depolarization. The major goal in our development of the CHT membrane depolarization assay is to establish an approach compatible with an HTS screen for allosteric CHT activators. Given the demonstration above that in CHT LV-AA stable cells staurosporine elevates CHT activity through a reduction in the choline K_M (Figure 4 and Table 1), we

dx.doi.org/10.1021/cn3000718 | ACS Chem. Neurosci. 2012, 3, 767–781

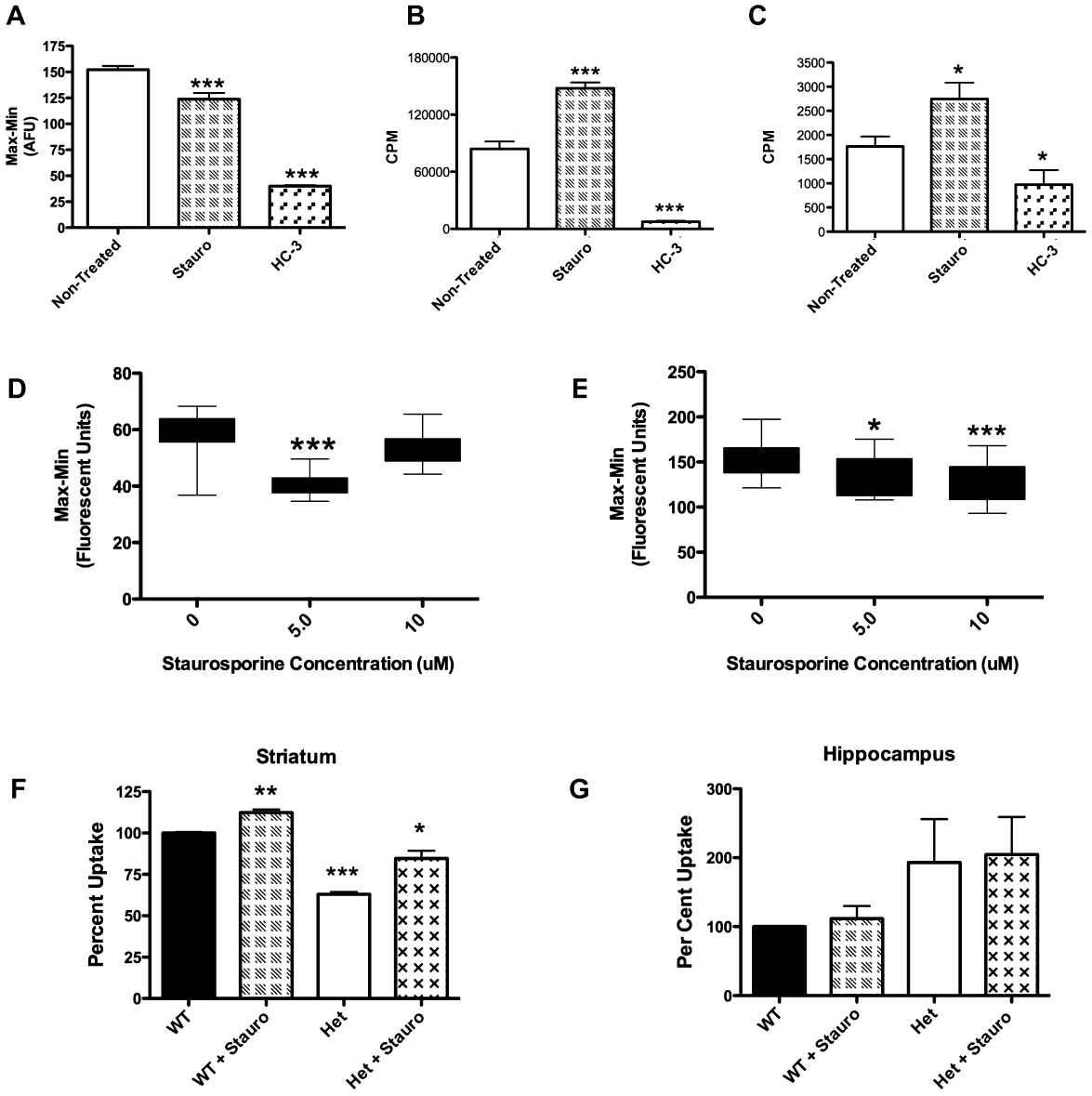

Figure 7. Establishment of secondary assays to verify compounds discovered using the choline-induced membrane potential assay: Staurosporine as a model CHT activator. (A–E) Secondary assays performed on the CHT LV-AA cell line. (A) The fluorescent peak response of the choline-induced membrane potential assay (bar 1) is inhibited by HC-3 (bar 3). Treatment of CHT LV-AA cells with 5 μM staurosporine for 60 s before choline application significantly reduced the fluorescent signal response mediated by Na+ flow through the transporter ($p < 0.0001$). (B) Following a successful HTS campaign, CHT active compounds will be initially screened for specificity through a traditional 3H-choline uptake assay adapted to a 96-well format (TopCount Perkin-Elmer). As shown in Figure 4 and Table 2, staurosporine was found to increase choline uptake through a K_M mechanism (210 nM choline, $p < 0.0001$). C) As an alternative, a real-time measurement of [^{3}H]-choline uptake in live cells via Scintillation Proximity Assay (SPA) may also be utilized, but this assay has a lower measured uptake signal. SPA results replicate the uptake finding ($p < 0.05$). (D–E) The concentration of applied choline impact response to compounds in the choline-induced membrane potential assay: (D) 5 μM, but not 10 μM, staurosporine treatment significantly decreased the membrane potential change induced with 410 nM choline ($p < 0.0001$). (E) Application of 10 μM choline produced a fluorescence response that was reduced in the presence of both 5 μM and 10 μM staurosporine. A greater reduction in fluorescent response is found treating with 10 μM staurosporine, although the 5 μM treatment is still significant ($p < 0.01$ and $p < 0.0001$). (F) Following verification in secondary assays, compounds found in this HTS campaign will be screened against prepared mouse synaptosomes. Staurosporine significantly increased the uptake of [^{3}H]-choline in mouse striatal synaptosomes ($p = 0.003$, $n = 3$, Student's t-test). The CHT heterozygous animal (±) could also be stimulated by staurosporine ($p = 0.01$) and demonstrated a reduced basal [^{3}H]-choline uptake capacity ($p < 0.001$). (G) In contrast, [^{3}H]-choline uptake measurements from hippocampal synaptosomes were staurosporine-insensitive. Although the CHT ± animal had an elevated uptake, this was not significant. Significant change was determined by Student's t-test analyses of all trials $n = 3–5$ for all assays and reported under values as *–*** for p values less than 0.05–0.001.

used staurosporine to test whether the fluorescence assay would report a comparable elevation in membrane potential (Figure 7A–C). We assessed choline-induced changes in membrane potential (Figure 7A) in parallel with a traditional uptake assay (Figure 7B), as well as in a scintillation proximity assay of choline uptake (Figure 7C), all in a 96-well format. In contrast to expectations, staurosporine (5 μM) decreased choline-induced changes in membrane potential, implying that fewer positively charged (likely Na^+) ions are moving through the transporter. These effects are CHT-dependent as staurosporine had no effect

dx.doi.org/10.1021/cn3000718 | ACS Chem. Neurosci. 2012, 3, 767–781

on the membrane potential of nontransfected cells (data not shown). The effect of staurosporine is apparent at low (420 nM), as well as high (30 μM), choline concentrations (Figure 7D,E) and is dose-dependent. Additionally, no significant inhibition of [^{3}H]-HC-3 binding was detected with staurosporine (data not shown). Thus, the CHT-dependent effects of staurosporine on membrane potential are most consistent with an allosteric action that shifts CHT to a high-affinity conformation that more efficiently couples choline uptake to the transmembrane sodium gradient at the expense of nonstoichiometric ion flow.[30] To our knowledge, the actions of staurosporine represent a novel mechanism by which a small molecule can potentiate the activity of an electrogenic transporter. Additionally, these results argue for consideration of both depolarizing and hyperpolarizing molecules when screening for activators of choline transport. Since we detected a choline K_M reduction with staurosporine treatments of both WT CHT and CHT LV-AA expressing cells (Table 1), agents with a profile such as that exhibited by staurosporine can be reasonably expected to stimulate choline transport activity in secondary assays using WT CHT.

Finally, to use the CHT LV-based membrane potential assay for HTS, we needed to establish the sensitivity and reliability of the assay from plate to plate and from day to day. The reproducibility and sensitivity of the assay can be assessed using a parameter termed Z′.[67] Values of Z′ greater than 0.5, obtained by assaying plates at three different times of the day on three sequential days, report that the assay is sensitive and reproducible enough to use for HTS paradigms. We compared EC_{20} (0.4 μM) versus EC_{max} (30 μM), obtaining Z′ values that yielded values of 0.52, 0.46, and 0.56 (data not shown). More recent studies using robotic application of choline in a 384-well format produced Z′ values ranging from 0.59 to 0.72 (Johns Hopkins Ion Channel Center, personal communication). These values support the utility of a membrane potential assay, in the context of an endocytosis-compromised CHT, for use in HTS activities. Since the majority of chemical libraries are dissolved and tested in DMSO, we determined the effects of DMSO in our assay. A final concentration of 0.1% or less had little to no effect on choline-induced membrane depolarization. Thus, our assay should permit a test of compounds at 10 μM in 0.1% DMSO, diluted from 10 mM stocks prepared in DMSO.

In summary, we have developed and characterized a novel membrane potential-based assay for CHT function that should permit the implementation of HTS screens for allosteric transporter modulators. The methods we are using currently for HTS of CHT inhibitors and activators is provided in Methods. The assay makes use of the endocytosis-limited CHT LV-AA mutant that produces much higher cell surface levels of CHT protein as well as significantly increased choline transport levels and CHT-dependent currents. In characterizing how agents used to study CHT regulation impact both WT CHT and CHT LV-AA, we discovered that staurosporine reduces choline K_M and increases choline flux at subsaturating choline concentrations. These changes are accompanied by a reduction in transporter-dependent, uncoupled ion flow, a result that has mechanistic significance in dissecting the processes by which ion-coupled choline flux relates to pathways of choline-gated, uncoupled ion flow. Our findings also have practical significance with respect to the use of the membrane potential assay to screen for CHT activators. Efforts to use HTS-based membrane potential assays for other electrogenic transporters should consider changes in substrate coupling and alterations in uncoupled ion flow into the selection of candidate modulators.

METHODS

Cell Culture. HEK-293T, HEK-293, and COS-7 cells were maintained according to ATCC guidelines and media recipes and used at 70−100% confluency. All mammalian cells were transfected using TransIT (Mirius) (according to the manufacturer's directions). Cells were harvested at 16−72 h growth according to the experimental design. HEK-293 cells stably expressing the human choline transporter (hCHT) or the hCHT mutant CHT LV-AA were selected from single cell colonies and maintained with media supplemented with 250 μg per mL of G418.

Plasmid Constructs. The eukaryotic expression vector pcDNA3 (Invitrogen) was used for expression studies in mammalian cell lines for CHT, Tac, and Tac-CHT fusion proteins. ChAT in PCMV6 was acquired from Origene, and Choline Kinase clones (CHKL and CHKA) were obtained from the Harvard Institute of Proteomics and recombined into HA-pLPCMV. Site-directed mutagenesis was performed according to the manufacturer's directions (Stratagene). All mutations were confirmed by double strand sequencing in the DNA Sequencing Core of the Vanderbilt Division of Genetic Medicine.

Tac Fluorescence Assay. Tac trafficking assays were performed as described in ref 40. Transfected, unpermeabilized HEK293 cells were labeled with anti-Tac antibody (1:250) at 4 °C for 1 h. The antibody was removed, fresh media applied, and the cells returned to 37 °C for 1 h. The cells were then fixed, permeabilized, and visualized with FITC conjugated mouse IgG staining (Rockland).

TAT-Peptide Analysis. HIV-TAT peptide sequence was synthesized as a fusion to hCHT sequence 524−539, corresponding to the 1° LV endocytic motif (Open Biosystems). The peptide was incubated with CHT HEK293 stable cell lines at 10 μM for 60 min followed by standard choline uptake measurement.

Na^+-Dependent Choline Uptake Assay. The activity and saturation kinetics of expressed CHT were assayed as described[29] with minor variation. For these studies, both COS-7 and HEK293 cells plated on poly-D-lysine coated plates were used as noted. Statistical analyses were performed using Student's *t*-test and One or Two Way Analysis of Variance using Graphpad Prism software (version 5.0).

Biotinylation of Surface Proteins. Cell surface biotinylations were performed as previously described[68] using NHS-S Biotin (Pierce). Biotinylated proteins were isolated with Ultralink Avidin (Pierce), eluted in Laemmli buffer, resolved by SDS−PAGE, blotted to PVDF membrane (Millipore), and probed with either the polyclonal rabbit (1:500−1:1000) or the monoclonal mouse CHT antibody (1:1000−1:5000) dependent upon experimental conditions. For MesNa cell stripping analysis, the following steps were added: biotinylated wells were returned to 37 °C for 5−15 min, then washed and incubated with MesNa (2-Mercaptoethanesulfonate) at 50 mM in PBS at 4 °C followed by three 15-min PBS washes before completion of the protocol. CHT antibodies have been described previously.[29,31,36]

Ooctye Physiology. Analysis of choline-activated currents in CHT cRNA-injected, *Xenopus laevis* ooctyes was performed by two-electrode voltage clamp as described in ref 30.

Choline-Induced Membrane Potential Assay (96-Well Flex-Station Format). HEK-293T cells stably expressing hCHT LV-AA or control cells were plated into 96 well, black walled, clear bottom poly-D-lysine coated plates (BioCoat BD Biosciences). Cells were plated in 50 μL/well at 70,000 cells/well and allowed to grow for 48 h. The cells were preincubated in HBSS/HEPES 1× dye (70 μL of Blue membrane potential dye, R8042 at 1.67 μg/mL, Molecular Devices) for 30 min. Tested compounds, such as staurosporine were also added at this preincubation step. The plates were read in FlexStation (Molecular Devices) to record baseline (1 min), and the FlexStation module was used to add choline (5×, 20 μL) at 0, 1, 5, and 10 μM final concentration in HBSS/HEPES 1× dye. Fluorescence was recorded for 2−4 min with sampling every 1.5 s. Data was analyzed by SoftMax Pro and exported to Excel for further analysis.

Choline-Induced Membrane Potential Assay (384-Well HTS Format). HEK-293T cells stably expressing CHT or CHT LV-AA or control cells were plated into 384-well, black walled, clear bottom poly-D-lysine coated plates (BioCoat BD Biosciences) at 20,000 cells in 20 μL/well dispensed using a Thermo Electron Multidrop reagent

dispenser. Plated cells grew overnight at 37 °C. The following day, the culture medium was removed and plates washed 3× with ELX washer (Biotek), and 20 μL/well of 1.67 μg/mL of the membrane potential dye (Molecular Devices #R8042) was added in assay buffer (Hanks Balanced Salt Solution (HBSS, Gibco) containing 20 mM HEPES, pH 7.3, by a dispenser (Thermo). Cells were incubated for 30 min at 37 °C. For agonist and antagonist screens, compounds are diluted to 2.5× their final desired concentration in HBSS. For control plates, a choline concentration curve and HC-3 were prepared in assay buffer at 5× the final concentration to be assayed. Cell plates and compound plates were loaded into a Hamamatsu FDSS 6000 kinetic imaging plate reader. The assay collected baseline fluorescence analysis for 20 s at 1/2 Hz prior to agonist/test compound addition. The selective CHT antagonist, HC-3, may be added or not, and the fluorescence was collected for an additional 2 min at 1/2 Hz, 10 μL of choline in assay buffer or choline plus agonist/test compound were added, and data were collected for an additional 7 min. Data were then analyzed by Hamamatsu FDSS 6000 imaging software and bulk export of collected data points to Excel for further analysis was immediately performed using spreadsheet software.

Scintillation Proximity Assay of Choline Uptake (96-Well Format). HEK-293T cells stably expressing hCHT LV-AA or control cells were plated at 125,000 cells in 100 μL/well and grown overnight. Each plate was washed two times with Kreb's–Ringer's–HEPES (KRH, and 20 mM HEPES buffer, pH 7.4). Wells were incubated with 40 μL of KRH buffer with or without drug at 1.25× using a Thermo dispenser. Plates were incubated at 37 °C in an atmosphere of 5% CO_2 for 15 min followed by an addition of a 10 μL volume of 205 nM or 410 nM (final concentrations) [^{3}H] choline chloride (Perkin-Elmer 1mCi/mL) in KRH buffer. Plates were incubated at 37 °C in an atmosphere of 5% CO_2 for 30 min, then cooled at room temperature for 15 min before sealing for readout in the TopCount (Perkin-Elmer).

Choline Transport Activity Assay (96-Well Format). HEK-293 cells stably expressing hCHT LV-AA or HEK293 control cells were plated into poly-D-lysine coated, 96 well, white, plates (Culturplate-96, Packard) at 75,000 cells in 100 μL/well and allowed to grow for 48 h. Each plate was washed two times with KRH and 20 mM HEPES buffer, pH 7.4. Wells were filled with 40 μL of KRH buffer with or without drug using a Thermo dispenser. Plates were incubated at 37 °C in an atmosphere of 5% CO_2 for 15 min followed by an addition of a 10 μL volume of 205 μM (final concentrations) [^{3}H]-choline chloride (Perkin-Elmer 1 mCi/mL) in KRH buffer and the assay completed as described previously. A volume of 100 μL of scintillant was used and plates analyzed by TopCount (Perkin-Elmer).

AUTHOR INFORMATION

Corresponding Author

*Suite 7140, MRBIII, Vanderbilt University School of Medicine, Nashville, TN 37232-8548. Tel: 615-771-0531. Fax: 615-936-3745. E-mail: randy.blakely@vanderbilt.edu.

Present Address

#Department of Cell Biology, Yale University, New Haven, CT 06510.

Author Contributions

Ruggiero, Ferguson, Iwamoto, Ivy, Holmstrand, Ennis, Weaver and Blakely participated in Research Design; Ruggiero, Wright, Ferguson, Lewis, Emerson, Iwamoto, Ivy, Holmstrand, and Ennis conducted experiments; Ruggiero, Wright, Ferguson, Lewis, Emerson, Iwamoto, Ivy, Holmstrand, and Ennis performed data analysis; Ruggiero, Ferguson, Holmstrand, Weaver and Blakely wrote or contributing to the writing of the paper.

Funding

MH073159 and a Zenith Award from the Alzheimer's Association (to R.D.B.) and MH078668 (to A.M.R.) supported our studies. Development of the non-Isotopic Screen for CHT was funded by the MLPCN Roadmap Initiative through NIDA 1 R03 DA028852-018 (to A.M.R. and R.D.B.) and performed at the Johns Hopkins Ion Channel Center (JHICC).

Notes

The authors declare no competing financial interest.

ACKNOWLEDGMENTS

We thank the Vanderbilt Institute of Chemical Biology High-Throughput Screening Center staff for their assistance and training in the development of this assay, the Vanderbilt Neuroscience Drug Discovery program and Craig Lindsley and Corey Hopkins for their assistance and expertise, members of the Blakely research group for their assistance and feedback throughout this project, and the Johns Hopkins Ion Channel Center for applying their talents and expertise in order to implement the HTS campaign, especially Min Li, Owen Thomas, and Meng Wu.

REFERENCES

(1) Marchbanks, R. M. (1975) Biochemistry and Cholinergic Neurons, in *Handbook of Psychopharmacology* (Iverson, L. L., Iverson, S. D., and Snyder, S. H., Eds.), pp 247–326, Plenum Press, New York.

(2) Sarter, M., and Parikh, V. (2005) Choline transporters, cholinergic transmission and cognition. *Nat. Rev. Neurosci. 6*, 48–56.

(3) Kasa, P. (1986) The cholinergic systems in brain and spinal cord. *Prog. Neurobiol. 26*, 211–272.

(4) Russell, R. W. (1982) Cholinergic system in behavior: the search for mechanisms of action. *Annu. Rev. Pharmacol. Toxicol. 22*, 435–463.

(5) Rowe, D. L., and Hermens, D. F. (2006) Attention-deficit/hyperactivity disorder: neurophysiology, information processing, arousal and drug development. *Expert Rev. Neurother. 6*, 1721–1734.

(6) Neumann, S. A., Lawrence, E. C., Jennings, J. R., Ferrell, R. E., and Manuck, S. B. (2005) Heart rate variability is associated with polymorphic variation in the choline transporter gene. *Psychosom. Med. 67*, 168–171.

(7) English, B. A., Appalsamy, M., Diedrich, A., Ruggiero, A. M., Lund, D., Wright, J., Keller, N. R., Louderback, K. M., Robertson, D., and Blakely, R. D. (2010) Tachycardia, reduced vagal capacity, and age-dependent ventricular dysfunction arising from diminished expression of the presynaptic choline transporter. *Am. J. Physiol. Heart Circ. Physiol. 299*, H799–810.

(8) Schmidt, C., Abicht, A., Krampfl, K., Voss, W., Stucka, R., Mildner, G., Petrova, S., Schara, U., Mortier, W., Bufler, J., Huebner, A., and Lochmuller, H. (2003) Congenital myasthenic syndrome due to a novel missense mutation in the gene encoding choline acetyltransferase. *Neuromuscul. Disord. 13*, 245–251.

(9) Soreq, H., and Seidman, S. (2001) Acetylcholinesterase–new roles for an old actor. *Nat. Rev. Neurosci. 2*, 294–302.

(10) Parihar, M. S., and Hemnani, T. (2004) Alzheimer's disease pathogenesis and therapeutic interventions. *J Clin Neurosci 11*, 456–467.

(11) Levy, M. L., Cummings, J. L., and Kahn-Rose, R. (1999) Neuropsychiatric symptoms and cholinergic therapy for Alzheimer's disease. *Gerontology 45* (Suppl 1), 15–22.

(12) Gilhus, N. E., Owe, J. F., Hoff, J. M., Romi, F., Skeie, G. O., and Aarli, J. A. (2011) Myasthenia gravis: a review of available treatment approaches. *Autoimmune Dis. 2011*, 847393.

(13) Wilens, T. E., and Decker, M. W. (2007) Neuronal nicotinic receptor agonists for the treatment of attention-deficit/hyperactivity disorder: focus on cognition. *Biochem. Pharmacol. 74*, 1212–1223.

(14) Sabbagh, M. N., Farlow, M. R., Relkin, N., and Beach, T. G. (2006) Do cholinergic therapies have disease-modifying effects in Alzheimer's disease? *Alzheimer's Dementia 2*, 118–125.

(15) Martorana, A., Esposito, Z., and Koch, G. (2010) Beyond the cholinergic hypothesis: do current drugs work in Alzheimer's disease? *CNS Neurosci. Ther. 16*, 235–245.

(16) Conn, P. J., Jones, C. K., and Lindsley, C. W. (2009) Subtype-selective allosteric modulators of muscarinic receptors for the treatment of CNS disorders. *Trends Pharmacol. Sci. 30*, 148−155.
(17) Bridges, T. M., LeBois, E. P., Hopkins, C. R., Wood, M. R., Jones, C. K., Conn, P. J., and Lindsley, C. W. (2010) The antipsychotic potential of muscarinic allosteric modulation. *Drug News Perspect. 23*, 229−240.
(18) Wilkinson, D. G., Francis, P. T., Schwam, E., and Payne-Parrish, J. (2004) Cholinesterase inhibitors used in the treatment of Alzheimer's disease: the relationship between pharmacological effects and clinical efficacy. *Drugs Aging 21*, 453−478.
(19) Mulder, A. H., Yamamura, H. I., Kuhar, M. J., and Snyder, S. H. (1974) Release of acetylcholine from hippocampal slices by potassium depolarization: dependence on high affinity choline uptake. *Brain Res. 70*, 372−376.
(20) Atweh, S., Simon, J. R., and Kuhar, M. J. (1975) Utilization of sodium-dependent high affinity choline uptake in vitro as a measure of the activity of cholinergic neurons in vivo. *Life Sci. 17*, 1535−1544.
(21) Simon, J. R., Atweh, S., and Kuhar, M. J. (1976) Sodium-dependent high affinity choline uptake: a regulatory step in the synthesis of acetylcholine. *J. Neurochem. 26*, 909−922.
(22) Guyenet, P., Lefresne, P., Rossier, J., Beaujouan, J. C., and Glowinski, J. (1973) Inhibition by hemicholinium-3 of (14C)-acetylcholine synthesis and (3H)choline high-affinity uptake in rat striatal synaptosomes. *Mol. Pharmacol. 9*, 630−639.
(23) Lowenstein, P. R., and Coyle, J. T. (1986) Rapid regulation of [3H]hemicholinium-3 binding sites in the rat brain. *Brain Res. 381*, 191−194.
(24) Freeman, J. J., Kosh, J. W., and Parrish, J. S. (1982) Peripheral toxicity of hemicholinium-3 in mice. *Br. J. Pharmacol. 77*, 239−244.
(25) Ferguson, S. M., Bazalakova, M., Savchenko, V., Tapia, J. C., Wright, J., and Blakely, R. D. (2004) Lethal impairment of cholinergic neurotransmission in hemicholinium-3-sensitive choline transporter knockout mice. *Proc. Natl. Acad. Sci. U.S.A. 101*, 8762−8767.
(26) Yamamura, H. I., and Snyder, S. H. (1972) Choline: high-affinity uptake by rat brain synaptosomes. *Science 178*, 626−628.
(27) Simon, J. R., and Kuhar, M. G. (1975) Impulse-flow regulation of high affinity choline uptake in brain cholinergic nerve terminals. *Nature 255*, 162−163.
(28) Kuhar, M. J., and Murrin, L. C. (1978) Sodium-dependent, high affinity choline uptake. *J. Neurochem. 30*, 15−21.
(29) Ferguson, S. M., Savchenko, V., Apparsundaram, S., Zwick, M., Wright, J., Heilman, C. J., Yi, H., Levey, A. I., and Blakely, R. D. (2003) Vesicular localization and activity-dependent trafficking of presynaptic choline transporters. *J. Neurosci. 23*, 9697−9709.
(30) Iwamoto, H., Blakely, R. D., and De Felice, L. J. (2006) Na+, Cl-, and pH dependence of the human choline transporter (hCHT) in Xenopus oocytes: the proton inactivation hypothesis of hCHT in synaptic vesicles. *J. Neurosci. 26*, 9851−9859.
(31) Misawa, H., Fujigaya, H., Nishimura, T., Moriwaki, Y., Okuda, T., Kawashima, K., Nakata, K., Ruggiero, A. M., Blakely, R. D., Nakatsu, F., and Ohno, H. (2008) Aberrant trafficking of the high-affinity choline transporter in AP-3-deficient mice. *Eur. J. Neurosci. 27*, 3109−3117.
(32) Salazar, G., Love, R., Werner, E., Doucette, M. M., Cheng, S., Levey, A., and Faundez, V. (2004) The zinc transporter ZnT3 interacts with AP-3 and it is preferentially targeted to a distinct synaptic vesicle subpopulation. *Mol. Biol. Cell 15*, 575−587.
(33) Schmidt, A., and Huttner, W. B. (1998) Biogenesis of synaptic-like microvesicles in perforated PC12 cells. *Methods 16*, 160−169.
(34) Apparsundaram, S., Ferguson, S. M., George, A. L., Jr., and Blakely, R. D. (2000) Molecular cloning of a human, hemicholinium-3-sensitive choline transporter. *Biochem. Biophys. Res. Commun. 276*, 862−867.
(35) Nakata, K., Okuda, T., and Misawa, H. (2004) Ultrastructural localization of high-affinity choline transporter in the rat neuromuscular junction: enrichment on synaptic vesicles. *Synapse 53*, 53−56.
(36) Holmstrand, E. C., Asafu-Adjei, J., Sampson, A. R., Blakely, R. D., and Sesack, S. R. (2010) Ultrastructural localization of high-affinity choline transporter in the rat anteroventral thalamus and ventral tegmental area: differences in axon morphology and transporter distribution. *J. Comp. Neurol. 518*, 1908−1924.
(37) Linding, R., Jensen, L. J., Diella, F., Bork, P., Gibson, T. J., and Russell, R. B. (2003) Protein disorder prediction: implications for structural proteomics. *Structure (Cambridge, MA, U.S.) 11*, 1453−1459.
(38) Evans, P. R., and Owen, D. J. (2002) Endocytosis and vesicle trafficking. *Curr. Opin. Struct. Biol. 12*, 814−821.
(39) Leonard, W. J., Depper, J. M., Crabtree, G. R., Rudikoff, S., Pumphrey, J., Robb, R. J., Kronke, M., Svetlik, P. B., Peffer, N. J., Waldmann, T. A., et al. (1984) Molecular cloning and expression of cDNAs for the human interleukin-2 receptor. *Nature 311*, 626−631.
(40) Tan, P. K., Waites, C., Liu, Y., Krantz, D. E., and Edwards, R. H. (1998) A leucine-based motif mediates the endocytosis of vesicular monoamine and acetylcholine transporters. *J. Biol. Chem. 273*, 17351−17360.
(41) Letourneur, F., and Klausner, R. D. (1992) A novel di-leucine motif and a tyrosine-based motif independently mediate lysosomal targeting and endocytosis of CD3 chains. *Cell 69*, 1143−1157.
(42) Ferguson, S. M., and De Camilli, P. (2012) Dynamin, a membrane-remodelling GTPase. *Nat. Rev. Mol. Cell Biol. 13*, 75−88.
(43) van der Bliek, A. M., Redelmeier, T. E., Damke, H., Tisdale, E. J., Meyerowitz, E. M., and Schmid, S. L. (1993) Mutations in human dynamin block an intermediate stage in coated vesicle formation. *J. Cell Biol. 122*, 553−563.
(44) Ferguson, S. M., and Blakely, R. D. (2004) The choline transporter resurfaces: new roles for synaptic vesicles? *Mol. Interventions 4*, 22−37.
(45) Apparsundaram, S., Ferguson, S. M., and Blakely, R. D. (2001) Molecular cloning and characterization of a murine hemicholinium-3-sensitive choline transporter. *Biochem. Soc. Trans. 29*, 711−716.
(46) Voglmaier, S. M., Kam, K., Yang, H., Fortin, D. L., Hua, Z., Nicoll, R. A., and Edwards, R. H. (2006) Distinct endocytic pathways control the rate and extent of synaptic vesicle protein recycling. *Neuron 51*, 71−84.
(47) Ehrlich, M., Boll, W., Van Oijen, A., Hariharan, R., Chandran, K., Nibert, M. L., and Kirchhausen, T. (2004) Endocytosis by random initiation and stabilization of clathrin-coated pits. *Cell 118*, 591−605.
(48) Blumstein, J., Faundez, V., Nakatsu, F., Saito, T., Ohno, H., and Kelly, R. B. (2001) The neuronal form of adaptor protein-3 is required for synaptic vesicle formation from endosomes. *J. Neurosci. 21*, 8034−8042.
(49) Salazar, G., Craige, B., Love, R., Kalman, D., and Faundez, V. (2005) Vglut1 and ZnT3 co-targeting mechanisms regulate vesicular zinc stores in PC12 cells. *J. Cell Sci. 118*, 1911−1921.
(50) Greengard, P., Valtorta, F., Czernik, A. J., and Benfenati, F. (1993) Synaptic vesicle phosphoproteins and regulation of synaptic function. *Science 259*, 780−785.
(51) Hvalby, O., Jensen, V., Kao, H. T., and Walaas, S. I. (2010) Synapsin-dependent vesicle recruitment modulated by forskolin, phorbol ester and ca in mouse excitatory hippocampal synapses. *Front. Synaptic Neurosci. 2*, 152.
(52) Leenders, A. G., and Sheng, Z. H. (2005) Modulation of neurotransmitter release by the second messenger-activated protein kinases: implications for presynaptic plasticity. *Pharmacol Ther 105*, 69−84.
(53) Gates, J., Jr., Ferguson, S. M., Blakely, R. D., and Apparsundaram, S. (2004) Regulation of choline transporter surface expression and phosphorylation by protein kinase C and protein phosphatase 1/2A. *J. Pharmacol. Exp. Ther. 310*, 536−545.
(54) Vogelsberg, V., Neff, N. H., and Hadjiconstantinou, M. (1997) Cyclic AMP-mediated enhancement of high-affinity choline transport and acetylcholine synthesis in brain. *J. Neurochem. 68*, 1062−1070.
(55) Knipper, M., Kahle, C., and Breer, H. (1992) Regulation of hemicholinium binding sites in isolated nerve terminals. *J. Neurobiol. 23*, 163−172.
(56) Sakrikar, D., Mazei-Robison, M. S., Mergy, M. A., Richtand, N. W., Han, Q., Hamilton, P. J., Bowton, E., Galli, A., Veenstra-Vanderweele, J., Gill, M., and Blakely, R. D. (2012) Attention deficit/hyperactivity disorder-derived coding variation in the dopamine transporter disrupts

microdomain targeting and trafficking regulation. *J. Neurosci. 32*, 5385−5397.
(57) Krantz, D. E., Waites, C., Oorschot, V., Liu, Y., Wilson, R. I., Tan, P. K., Klumperman, J., and Edwards, R. H. (2000) A phosphorylation site regulates sorting of the vesicular acetylcholine transporter to dense core vesicles. *J. Cell Biol. 149*, 379−396.
(58) Rao, A., Richards, T. L., Simmons, D., Zahniser, N. R., and Sorkin, A. (2012) Epitope-tagged dopamine transporter knock-in mice reveal rapid endocytic trafficking and filopodia targeting of the transporter in dopaminergic axons. *FASEB J. 26*, 1921−1933.
(59) Holton, K. L., Loder, M. K., and Melikian, H. E. (2005) Nonclassical, distinct endocytic signals dictate constitutive and PKC-regulated neurotransmitter transporter internalization. *Nat. Neurosci. 8*, 881−888.
(60) Cheng, Y., and Prusoff, W. H. (1973) Relationship between the inhibition constant (K1) and the concentration of inhibitor which causes 50% inhibition (I50) of an enzymatic reaction. *Biochem. Pharmacol. 22*, 3099−3108.
(61) Chatterjee, T. K., Cannon, J. G., and Bhatnagar, R. K. (1987) Characteristics of [3H]hemicholinium-3 binding to rat striatal membranes: evidence for negative cooperative site-site interactions. *J. Neurochem. 49*, 1191−1201.
(62) Sandberg, K., and Coyle, J. T. (1985) Characterization of [3H]hemicholinium-3 binding associated with neuronal choline uptake sites in rat brain membranes. *Brain Res. 348*, 321−330.
(63) Okuda, T., Konishi, A., Misawa, H., and Haga, T. (2011) Substrate-induced internalization of the high-affinity choline transporter. *J. Neurosci. 31*, 14989−14997.
(64) Suhre, W. M., Ekins, S., Chang, C., Swaan, P. W., and Wright, S. H. (2005) Molecular determinants of substrate/inhibitor binding to the human and rabbit renal organic cation transporters hOCT2 and rbOCT2. *Mol. Pharmacol. 67*, 1067−1077.
(65) Muller, J., Lips, K. S., Metzner, L., Neubert, R. H., Koepsell, H., and Brandsch, M. (2005) Drug specificity and intestinal membrane localization of human organic cation transporters (OCT). *Biochem. Pharmacol. 70*, 1851−1860.
(66) Sweet, D. H., Miller, D. S., and Pritchard, J. B. (2001) Ventricular choline transport: a role for organic cation transporter 2 expressed in choroid plexus. *J. Biol. Chem. 276*, 41611−41619.
(67) Zhang, J. H., Chung, T. D., and Oldenburg, K. R. (1999) A simple statistical parameter for use in evaluation and validation of high throughput screening assays. *J. Biomol. Screening 4*, 67−73.
(68) Ruggiero, A. M., Liu, Y., Vidensky, S., Maier, S., Jung, E., Farhan, H., Robinson, M. B., Sitte, H. H., and Rothstein, J. D. (2008) The endoplasmic reticulum exit of glutamate transporter is regulated by the inducible mammalian Yip6b/GTRAP3−18 protein. *J. Biol. Chem. 283*, 6175−6183.
(69) Li, H., Waites, C. L., Staal, R. G., Dobryy, Y., Park, J., Sulzer, D. L., and Edwards, R. H. (2005) Sorting of vesicular monoamine transporter 2 to the regulated secretory pathway confers the somatodendritic exocytosis of monoamines. *Neuron 48*, 619−633.